# Fast spectral variability of the RS CVn-type chromosphere-active star II Peg

B. Zhilyaev, M. Andreev, I. Verlyuk
Main Astronomical Observatory of National Academy of Sciences of Ukraine, Kiev
zhilyaev@mao.kiev.ua

(Submitted on 16 May 2023; Accepted on 27 June 2023)

**Abstract.** We discuss the detection of fast spectral variability of II Peg in the subsecond range. Spectral observations were carried out with a grism spectrograph on a 60 cm telescope at Peak Terskol on August 9 - 10, 2010. The low-resolution spectra (R $\sim$ 100) were obtained with an exposure time of 1.5 s. Estimates of the UBV magnitudes were obtained by mathematical convolution of the spectra with filter transmission curves. The flares follow continuously at a rate of about one event per minute. The amplitude of the flares in the U band averages about 0.25 mags. We have detected a periodic signal that controls the light curves of the II Peg flare, a 77-second high-frequency oscillation (HFO) with an amplitude of about 0.05 magnitude. We found that the flares are caused by HFO maxima. The colourimetric analysis shows that at maximum brightness the flares emit as a black body in the temperature range from 12 000 to 35 000 K. The linear size of a flare with a temperature of 12 100 K is approximately 3.9 % of the star's radius. The colourimetric analysis also shows that in the process of brightness fluctuations, the flare plasma oscillates between the states of optically thin and optically thick in the Balmer continuum.

**Key words:** stars: activity – stars: flare – stars: chromospheres – methods: observational –

## Introduction

RS Canum Venaticorm (RS CVn) type stars are chromospherically active binary systems with large starspots, vast chromospheric plages. They produce strong flares observable at all wavelengths. II Peg (HD 224085) is one of the most active RS CVn stars. II Peg is a binary star system with V $\sim$ 7.37. The primary is a cool K-type subgiant. The smaller companion is a red M-type dwarf tidally locked in an orbit with a period of 6.7 days. II Peg displays evidence for starspots covering a fraction of the photosphere up to 40 %.

Doppler images of II Peg based on two data sets obtained in 2004 February and November show a wide latitude distribution of starspots. Most spots are concentrated at a high-latitude belt above 60° and a low-latitude belt near the equator. The starspots evolved dramatically between two observing runs (Yue Xiang et al. 2014).

The Doppler imaging maps show the mean $T_{\rm eff}$ from 4500 to 4700 K, the temperature of the coolest spot structure is usually about 3500–4000 K (Hackman et al. 2012).

Mathioudakis et al. (2003) report the intensity oscillations detected in the Johnson $U$-band during a flare on II Peg in August 1989 using the 0.75m Cassegrain reflector. FFT analysis reveals a period of 220 s. Oscillating coronal loop models were used to derive physical parameters such as temperature, electron density and magnetic field strength associated with the coronal loop. Assuming an aspect ratio of 0.25 (often seen in solar two ribbon flares), a loop length of $L \sim 5 \cdot 10^{10}$ cm can be derived. The periodicities observed have been interpreted in terms of Alfven oscillations of a coronal loop (Zaitsev & Stepanov 1989). The extensive analysis of the II Peg flare revealed physical parameters of the flare plasma: $T = 2 \cdot 10^8$ K, $n_e = 4 \cdot 10^{11}$ cm$^{-3}$, $B = 600$

Gauss. The energy of the flare event in optical wavelengths was in excess of $10^{36}$ erg.

The observation by the Swift X-ray Telescope during a large flare on II Peg represents detections of photospheric Fe K-alpha from a star (Ercolano et al. 2008). The flaring-loop models constrain the maximum height of a flare to 0.15 $R_*$. Using results of flaring-loop models, the authors estimate a flare loop height of 0.13 $R_*$, plasma density of $\sim 4 \cdot 10^{11}$ cm$^{-3}$, and emitting volume of $\sim 6 \cdot 10^{30}$ cm$^3$. Adopting a radius for II Peg of 3.4 $R_\odot$ (Berdyugina et al. 1998), this loop half-length corresponds to a loop height of 0.13 $R_*$. These estimates for the flare dimensions and density allow estimating the average energy output of the large flare to be $\sim 10^{33}$ s$^{-1}$, or 1/10th of the stellar bolometric luminosity. The estimation for the conductive energy losses is $\sim 10^{33}$ erg.

High-resolution echelle optical spectroscopy of II Peg shows strong emission of Ca II H & K and absorption of Na D1 and D2 lines (Ajaz Ahmad Dar et al. 2018). The EWs of Ca II K and Ca II H indicates variations over 1.3 Å. It is assumed this may be likely due to flares.

We discuss the detection of fast spectral variability of II Peg in the subsecond range.

## Observations and data processing

This section presents the results of fast spectrophotometry of flares on the flare star II Peg with a grism spectrograph (Zhilyaev et al. 2012).

The spectral monitoring of II Peg ($U = 9.06$, $U - B = 0.68$, $B - V = 1.02$) was carried out with a slitless spectrograph on August 9 - 10, 2010. The Zeis-600 telescope was used at the Peak Terskol Observatory with spectral resolution of R $\sim$ 100. Fig. 1 shows the time series of 344 spectra of II Peg and a comparison star with an exposure time of 1.5 sec and a time resolution of 3.057 sec. Estimates of the $UBV$ magnitudes and light curves (Fig. 3) were obtained by mathematical convolution of the spectra with filter transmission curves.

A fragment of the small-scale fast variability II Peg obtained with a high-speed two-channel photometer on a 2-m telescope on August 8, 2010, at Terskol Peak is shown in Fig. 4. We can see flashes with a period of about 100 seconds.

Fig. 2 shows variations in the spectra of II Peg during a flare. Similar data are also given for the comparison star. It is easy to see that during the flare, additional emission appears in the II Peg spectrum in the Balmer line $H_\gamma$, Ca II H, K, Mg b. Variations in the spectrum of the comparison star are not observed.

Next, we present a detailed photometric and colorimetric analysis that allows us to evaluate the important characteristics of the II Peg flares: temperature at maximum brightness and its size.

## Properties of high-frequency variations in flares

Fig. 3 shows II Peg light curves in $UBV$ filters. During the measurement, approximately 10 flares occurred, on average one flash in 74 seconds. The

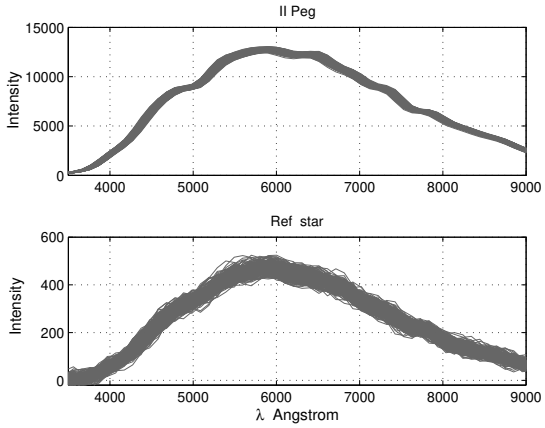


**Fig. 1.** The spectra of II Peg and ref star

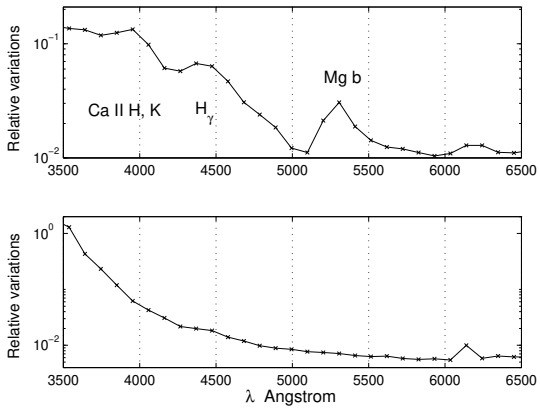


**Fig. 2.** Variations in spectra.

duration of flares averages around 60 seconds. But sometimes there are very short flares lasting a few seconds, which is appropriate to call "lightning".

Figures 3, 4 and 5 show flashes follow continuously at a frequency of about one flash per minute. The flare amplitude in the $U$-band averages about 0.25 magnitude.

## Flare colorimetry

The modern approach to colorimetry is based on multicolor $UBVRI$ spectrophotometry in the spectral region from about of 3500 to approximately of 9000 Å. Colorimetry is a quantitative method for analyzing radiation. It allows

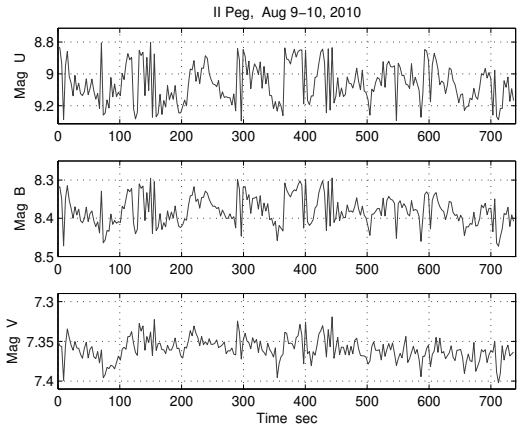


**Fig. 3.** $UBV$ light curves of II Peg on August 9 - 10, 2010.

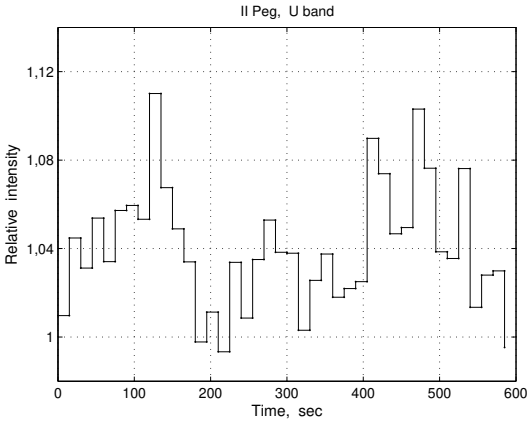


**Fig. 4.** A fragment of the small-scale fast variability II Peg obtained on a 2-m telescope at Peak Terskol on August 8, 2010.

one to diagnose the radiation of a celestial body, determine the temperature, electron concentration, optical thickness of the emitting plasma based on theoretical diagnostic color diagrams calculated for various radiation sources.

At first, in each filter the intensities $FU_0, FB_0, FV_0$ in a quiet state of a star were calculated in Fig. 3. Then these values were subtracted from the corresponding values $FU, FB, FV$ of the flare intensities. Based on the obtained residues, the color indices of the intrinsic emission of the flare were determined:

$$U - B = -2.5 \lg \left[ \frac{FU - FU_0}{FB - FB_0} \right] + \triangle_{UB} \qquad (1)$$

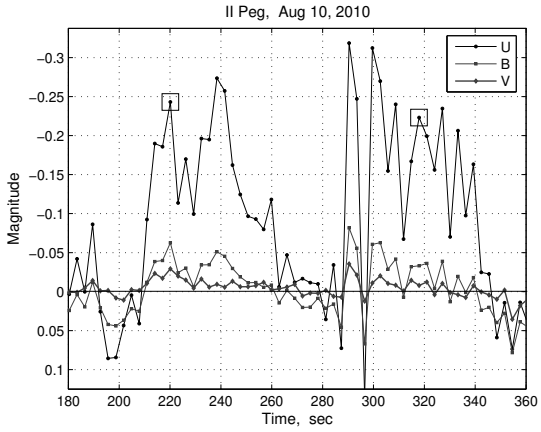


**Fig. 5.** Fragment of the $UBV$ light curves II Peg. The squares mark the brightness maxima of the flares that lie on the emission line of a black body in Fig. 6.

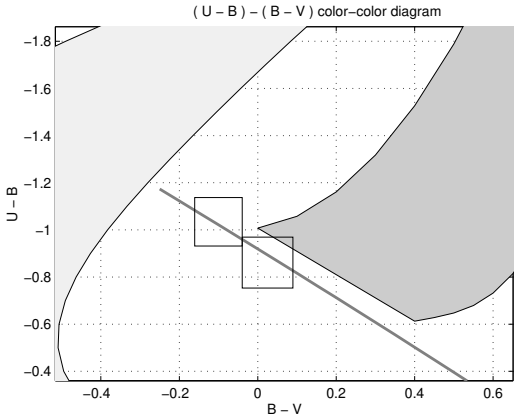


**Fig. 6.** Colors of points of Fig. 5 on the $(U-B)$ - $(B-V)$ diagram. The 1-sigma error squares are given. The bottom strong line indicates the radiation of a black body.

$$B-V=-2.5\lg\left[\frac{FB-FB_0}{FV-FV_0}\right]+\triangle_{BV} \qquad (2)$$

where $\triangle_{UB}=0.68+2.5\lg\frac{FU_0}{FB_0}$, $\triangle_{BV}=1.02+2.5\lg\frac{FB_0}{FV_0}$ are normalization coefficients. These coefficients take into account the color indices of the star in a quiet state: $U-B=0.68$, $B-V=1.02$.

To develop two-color diagrams, we used the color indices of various radiation sources (Straizys 1977; Chalenko 1999). The bright area of the diagram $(U-B)$ - $(B-V)$ in Fig. 6 corresponds to the color characteristics of a hydro-

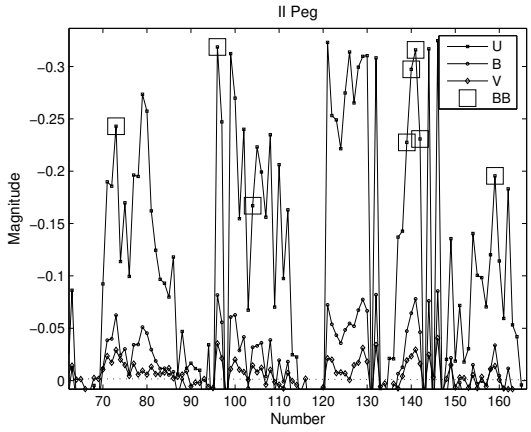


**Fig. 7.** Fragment of the $UBV$ light curves II Peg on August 10, 2010. The squares mark the series of brightness maximums of the flares that lie on the emission line of a black body in Fig. 8.

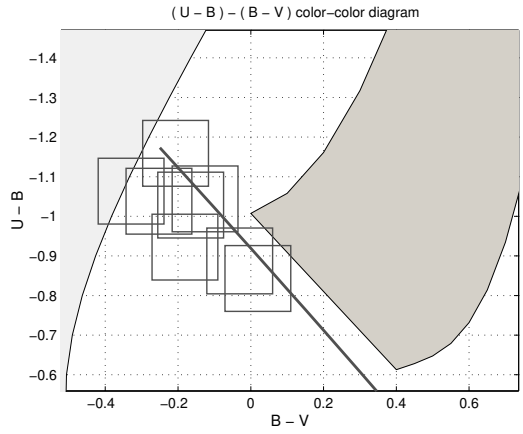


**Fig. 8.** Colors of points of Fig. 7 on the $(U-B)$ - $(B-V)$ diagram. The 95 % error squares are given. The bottom strong line indicates the radiation of a black body.

gen plasma that is optically thin in the Balmer continuum with $T_e \sim 10\,000$ K and $N_e$ from $10^{14}$ to $10^{10}$ cm$^{-3}$. The dark region of the diagram corresponds to an optically thick plasma with $T_e$ from 15 000 to 8 000 K. Blackbody radiation is indicated by the bottom bold line.

The squares in Fig. 6 show two flares on the blackbody emission line with temperatures of $12\,100 \pm 200$ K and $18\,900 \pm 800$ K. They correspond to two flares in Fig. 5 marked with a square at the brightness maxima.

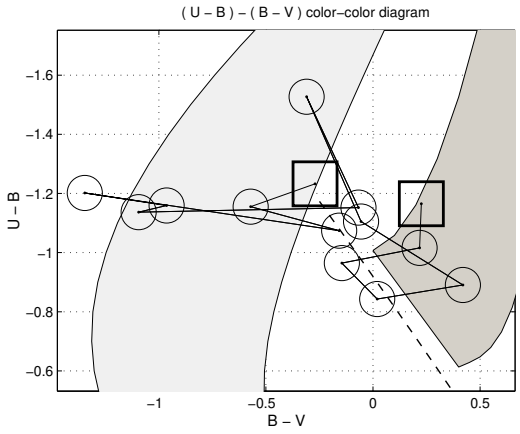


**Fig. 9.** Color tracks on the $(U-B)$ - $(B-V)$ diagram. The 1-sigma error ellipses are given. The bottom dashed line indicates the radiation of a black body. The squares indicate the position of the flare beginning and flare end.

Fig. 7 shows a fragment of the $UBV$ light curve of II Peg. The squares mark the series of brightness maximums of the flares that lie on the emission line of a black body in Fig. 8. At maximum brightness, flashes emit like a black body in the temperature range from 12 to 35 thousand K.

Fig. 9 shows the temporal evolution of the color characteristics of a flare (points 70 to 83 in Fig. 7). 95 % error ellipses of the color characteristics are shown. Ellipses on tracks follow with a time step of 3.057 seconds. Color errors are calculated for Poisson flows of quanta.

It is easy to see that the flare begins in the region of optically thick plasma and ends in the region of the optically thin plasma. Five points on the light curve lie on the emission line of a black body. Colorimetric analysis shows that in the process of brightness fluctuations, the flare plasma oscillates between the states of optically thin and optically thick in the Balmer continuum

## Flares sizes

The flare luminosity in the $U$-band can be determined by convolving the spectrum of a black body with the transmission curve of the $U$ filter. Flare area $s$ can be defined as (Alekseev et al. 1997):

$$\frac{s}{S} = \left(10^{0.4\triangle U} - 1\right) \frac{FU_0}{FU} \tag{3}$$

where $S$ is the area of the visible disk of the star, $\triangle U$ is the amplitude of the flare in the $U$-band, $FU_0$ and $FU$ are the Planck function of the photosphere and flare with effective temperature $T_{bb}$:

$$F(T_{bb}) = \int \frac{U(\lambda)}{\lambda^5} \left[\exp\left(\frac{1.4388}{\lambda T_{bb}} - 1\right)\right] d\lambda \tag{4}$$

Here $U(\lambda)$ is the transmission curve of the $U$ filter. Knowing the observed flare amplitude in the $U$-band, the photosphere temperature of II Peg 4600 K (Hackman et al. 2012), and the temperature at the maximum of the flare, one can easily estimate the size of the flare using the above formulas.

The linear size of the flare in Fig. 6 with a temperature of 12 100 K and amplitude in the $U$-band equal to 0.25 mag at the maximum luminosity is approximately 3.9 % of the radius of the star or about 0.15 % of the area of the visible disk of the star. Adopting a radius for II Peg of 3.4 $R_\odot$ (Berdyugina et al. 1998), the linear size of the flare $a$ equals 9.5 $\cdot 10^9$ cm.

The linear size of the flare in Fig. 7 with a temperature of 35 000 K is approximately 1.1 % of the radius of the star or about 0.012 % of the area of the visible disk of the star.

## Diagnostics of coronal plasma

To estimate the main parameters of the flare plasma and magnetic field we use the solar-stellar analogy and a diagnostic method developed taking into account the characteristics of dispersion, excitation and attenuation of eigenmodes of vibration of magnetic tubes. Key assumptions of the models proposed by Stepanov et al. (2005) are as follows. The coronal loop can be presented in the form of a cylinder with firmly fixed bottoms. A sharp increase in gas pressure in an outburst can cause fast magneto acoustic (FMA) modes, the period of which is determined by tube cross-section $a$. If the coronal arc acts as a magnetic trap and can collect charged particles, the FMA oscillations will lead to modulation of accelerated particle flux in the chromosphere and photosphere due to a change in coefficient stuck. The thermalization of particles leads to the observed pulsations of the optical radiation.

In terms of the scenario described by Stepanov et al. (2005), we give formulas for estimating the temperature $T$, particle concentration $n$ and magnetic field $B$ in the contour of the flare, using the following parameters of radiation oscillations: period $T_p$, modulation depth $M$, $Q$ factor $Q = 2\pi\tau/T_p$, $a$ and $L$ - radius and length of magnetic tube.

The approach of Stepanov et al. (2005) made it possible to obtain relations for determining parameters of flare plasma in the coronal loop:

$$T \approx 2.4 \times 10^{-8} \frac{\tilde{r}^2 M}{T_p^2 \chi} \ \ [\mathrm{K}],$$

$$n \approx 1.97 \times 10^{-12} \frac{\tilde{r}^3 \tilde{\kappa} M^{5/2} Q \sin^2\theta}{T_p^4 \chi^{3/2}} \ \ [\mathrm{cm}^{-3}],$$

$$B \approx 9.06 \times 10^{-18} \frac{Q^{1/2} \tilde{r}^{5/2} \tilde{\kappa}^{1/2} M^{5/4} \sin\theta}{T_p^3 \chi^{5/4}} \ \ [\mathrm{G}].$$

where $\theta \approx \mathrm{arctg}(\eta_0 a/\pi L)$ is the angle between the FMA wave vector $\mathbf{k}$ and the magnetic field $\mathbf{B}$, $\tilde{r} = 2\pi a/\eta_0$, $\eta_0 \approx 2.4$, $\chi = 20/3M + 2$, $\tilde{\kappa} = 486M\cos^2\theta + 1$.

The quality factor $Q$ is a parameter of the oscillatory system, which characterizes a loss of energy when the phase increases by 1 radian. The $Q$ factor is related to the logarithmic decrement $\lambda$ by the relation

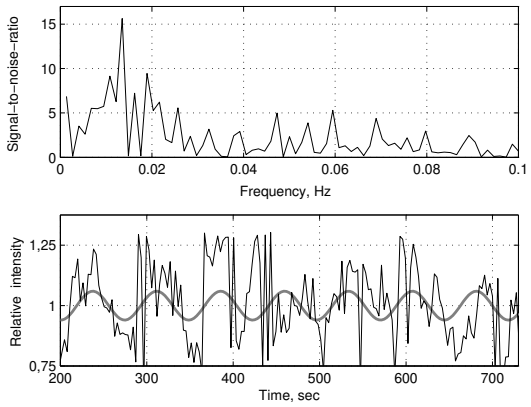


**Fig. 10.** FFT power spectra of the $U$-band light curve (top panel) and $U$-band light curve of the II Peg flare (bottom panel). The HFO curve is highlighted in bold.

$$Q = \frac{2\pi}{1 - e^{-\lambda}}$$

To determine the value of $Q$, we calculate the logarithmic decrement $\lambda$ according to the formula

$$\lambda = \frac{1}{n} \ln \frac{x(t)}{x(t + nT_p)}$$

where $n$ is an integer of positive peaks in the light curve.

The modulation depth $M \simeq 0.1$ and $Q$ factor $\simeq 57$ can be determined from the $U$-band light curve in Fig. 10. The oscillation period $T_p$ of the high-frequency oscillation (HFO) light curve equal to about 77 sec can be derived from the FFT power spectrum in Fig. 10.

Given the results of observations of flares on II Peg: assuming an aspect ratio of 0.25 (often seen in solar flares), and $a \simeq 1 \cdot 10^{10}$ cm a loop length of $L \simeq 4.0 \cdot 10^{10}$ cm can be derived. Taking the values $Tp$, $M$, $Q$, given above, we obtain the values of temperature, concentration of particles and magnetic field strength in the plasma of the coronal loop: $T \approx 3.2 \cdot 10^8$ K, $n \approx 2.2 \cdot 10^{11}$ cm$^{-3}$, $B \approx 1106$ G.

Note that the extensive analysis of the II Peg flare reported by Mathioudakis et al. (2003), revealed physical parameters of the flare plasma: $T = 2 \cdot 10^8$ K, $n = 4 \cdot 10^{11}$ cm$^{-3}$, $B = 600$ G.

## Conclusion

The results of the photometric analysis of flares on the RS CVn star II Pegasi are presented. The spectral monitoring of II Peg was carried out with a slitless

spectrograph on August 9 - 10, 2010. The Zeis-600 telescope was used at the Peak Terskol Observatory with a spectral resolution of R $\sim$ 100. Estimates of the $UBV$ light curves were obtained by mathematical convolution of the spectra with filter transmission curves.

We found a periodic signal that controls the flare light curves of II Peg, a 77 s HFO in the $U$-band light curve with an amplitude of about 0.05 mag. We believe the HFO could be a property of the flaring loop. As can be seen, the flares can be triggered by HFO maxima.

Flare colourimetry of the flare series reveals flares in brightness maxima emit like a black body in the temperature range from 12 to 35 thousand K.

The linear size of the flares, depending on temperature, ranges from about 4 % to about 1 % of the radius of the star. The linear size of a flare with a temperature of about 12 000 K is about $1 \cdot 10^{10}$ cm.

We estimate the main parameters of small-scale II Peg flares based on the solar-stellar analogy using the model proposed by Stepanov et al. (2005). Taking into account the results of observations of flares on II Peg, we obtain the values of temperature, particle density, and magnetic field strength in the coronal plasma for an ordinary flare: $T \approx 3.2 \cdot 10^8$ K, $n \approx 2.2 \cdot 10^{11}$ cm $^{-3}$, $B \approx 1106$ G.

## References

Ajaz Ahmad Dar, et al. 2018, Res. Astron. Astrophys. 18, 112
Alekseev, I., & Gershberg, R. 1997. *The Earth and the Universe*. Asteriadis, G. (Ed.). Aristotle Univ. Thessaloniki: Ziti Edition. 53
Berdyugina, S., Jankov, S., Ilyin, I., et al. 1989, A&A, 334, 863
Chalenko, N. 1999, Astronomy Reports, No. 7, 459
Ercolano, B., Drake, J., Reale, F., et al. 2008, ApJ, 688, 1315
Hackman, T., Mantere, M., Lindborg, M., et al., 2012, A&A, 538, A126
Mathioudakis, M., Seiradakis, J., Williams, D., et al. 2003, A&A 403, 1101
Stepanov, A.V., Kopylova, Yu.G., Tsap, Yu.T., et al. 2005, Letters to Astron. Journal, 31, 684
Straizys, V. 1977, *Multicolor Stellar Photometry*. Vilnius: Mokslas Publishers
Yue Xiang, Sheng-hong Gu, A. Collier Cameron, et al. 2014, MNRAS 438, 2307
Zaitsev, V.V., & Stepanov, A.V. 1989, Sov. Astron. Lett., 15, 6
Zhilyaev, B., Andreev, M., Sergeev, A. et al. 2012, Astronomy Letters, 38, No. 12, 793